The 21st International Congress on Sound and Vibration

13-17 July, 2014, Beijing/China

Analysis of Modal Frequencies of Tubes with Internal Constriction Using the Blockage Integral

Mukherjee, Nalini and Heckl, Maria

School of Computing and Mathematics, Keele University, U.K.

e-mail: n.mukherjee@keele.ac.uk

The aim of this paper is to study two similar combustor designs: one with a small blockage and other with a larger blockage. We model the blockage as a lumped inertia and calculate its effective length by using the concept of the 'Blockage Integral'. The integration is performed along a path in a hypothetical potential flow field in the combustor. The change of blockage integral with fluctuation of blockage size will be observed. Subsequently, the eigen frequencies of the system will be evaluated and their variations with physical parameters like blockage size/profile, blockage location within tube and jump in cross-sectional area will be observed. The impact of different boundary conditions at tube ends will also be taken care of, as part of our case studies. Our present analysis assumes constant temperature within the tube.

1. Introduction

The present work focuses on the acoustic behaviour of tubes with internal blockage. A special parameter called 'blockage integral' is going to be introduced to quantify the effect of the blockage inside the tube. The idea behind the blockage integral is to represent the physical blockage as an acoustic lumped mass. Thus the analysis is applicable to low frequencies alone. The idea of the blockage integral has been adopted from the earlier work of Heckl and Howe[1], where a stability analysis for the Rijke tube has been performed with a Green's function approach. The works of Murray and Heckl[2] as well as Murray and Howe[3] deal with the Green's function model of rectangular tube and generic Rijke burner. They included the concept of effective length of blockage in their work. Previous works from Flohr et al[4, 5] dealt with CFD analysis of premixed flames and gas turbine burner transfer functions. The idea of effective length of blockage has been observed there, as well. However, a detailed analysis of modal frequencies for a tube with blockage using the concept of blockage integral has never been done before. Moreover, in this piece of work, the variation of modal frequencies with tube blockage and area jump is going to be examined in detail. At the final stage, we are going to have a look at the pressure profile within the system and try to understand the reason of the tube system response with respect to change in area jump or blockage value.

2. Mathematical model

We begin with a generalised model of a tube with area jump and blockage inside. A schematic representation is shown in fig 1. The tube has got an area jump from S_1 to S_2 at $x = x_1$, and a blockage at $x = x_2$.

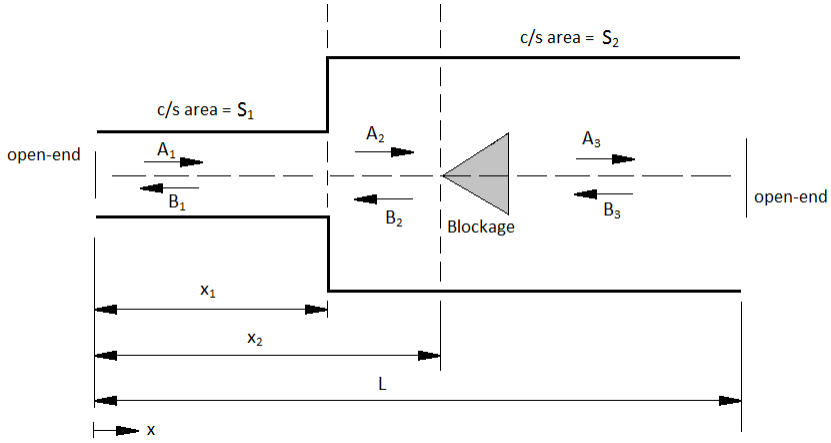

Fig 1: Schematic of a tube with area jump and blockage inside

In order to model this mathematically, we divide the tube into three distinct zones (see figure 1) and assume 1-D acoustic waves in each zone. The pressure and velocity are written in terms of the 6 undetermined amplitudes A_1, A_2, A_3 (forward travelling waves) and B_1, B_2, B_3 (backward travelling waves).

$$p_1(x,t) = (A_1 e^{-jkx} + B_1 e^{jkx}) e^{j\omega t}, \quad u_1(x,t) = (1/\rho c)(A_1 e^{-jkx} - B_1 e^{jkx}) e^{j\omega t} \quad \text{for } 0 < x < x_1 \tag{1}$$

$$p_2(x,t) = (A_2 e^{-jkx} + B_2 e^{jkx}) e^{j\omega t}, \quad u_2(x,t) = (1/\rho c)(A_2 e^{-jkx} - B_2 e^{jkx}) e^{j\omega t} \quad \text{for } x_1 < x < x_2 \tag{2}$$

$$p_3(x,t) = (A_3 e^{-jkx} + B_3 e^{jkx}) e^{j\omega t}, \quad u_3(x,t) = (1/\rho c)(A_3 e^{-jkx} - B_3 e^{jkx}) e^{j\omega t} \quad \text{for } x_2 < x < L \tag{3}$$

ρ is the density, c is the speed of sound and k is the wave number ($=\omega/c$).

At the interfaces between the three zones, we assume conservation of mass and momentum

At $x = x_1$ $\quad p_1(x,t) = p_2(x,t)$ and

$$S_1 u_1(x,t) = S_2 u_2(x,t) \tag{4}$$

At $x = x_2$ $\quad p_2(x,t) - p_3(x,t) = \rho_2 L_{eff} \left(\partial u_2(x,t)/\partial t\right)$ and

$$u_2(x,t) = u_3(x,t) \tag{5}$$

The concept of L_{eff} will be discussed in the section 4 in more detail.

We assume that the tube ends are open and can be described by pressure release boundary conditions,

$$p_1(x,t) = 0, \text{ at } x = 0 \tag{6}$$

$$p_3(x,t) = 0, \text{ at } x = L \tag{7}$$

3. Calculation of eigen-frequencies

To calculate the eigen-frequencies, we use equations (1)-(7). These can be written as a matrix equation,

$$\begin{bmatrix} 1 & 1 & 0 & 0 & 0 & 0 \\ e^{-jkx_1} & -e^{jkx_1} & -\overline{\rho c}\overline{S}e^{-jkx_1} & \overline{\rho c}\overline{S}e^{jkx_1} & 0 & 0 \\ e^{-jkx_1} & e^{jkx_1} & -e^{jkx_1} & -e^{jkx_1} & 0 & 0 \\ 0 & 0 & e^{-jkx_2} & -e^{jkx_2} & -\overline{\rho c}e^{-jkx_2} & \overline{\rho c}e^{jkx_2} \\ 0 & 0 & (1-jL_{eff}\omega/c)e^{-jkx_2} & (1+jL_{eff}\omega/c)e^{jkx_2} & -e^{-jkx_2} & -e^{jkx_2} \\ 0 & 0 & 0 & 0 & e^{-jkL} & e^{jkL} \end{bmatrix} \begin{Bmatrix} A_1 \\ B_1 \\ A_2 \\ B_2 \\ A_3 \\ B_3 \end{Bmatrix} = \begin{Bmatrix} 0 \\ 0 \\ 0 \\ 0 \\ 0 \\ 0 \end{Bmatrix} \quad (8)$$

The characteristic equation is obtained by equating the determinant of the above 6×6 matrix to zero. It has the form $f(k)=0$, where

$$f(k)=\sin k(L-x_1)\cos kx_1+\overline{S}\sin kx_1\cos k(L-x_1)+L_{eff}k\cos k(L-x_2)\left[\cos kx_1\cos k(x_2-x_1)+\overline{S}\sin kx_1\sin k(x_1-x_2)\right] \quad (9)$$

$\overline{S}=S_2/S_1$ is the ratio of the cross sectional areas

The special cases of this model are;

i. there is no area jump or,
ii. the blockage location and area jump location coincide.

The characteristic equation has to be solved numerically, e.g. by using the Newton-Raphson method, to determine the allowed values of 'k' or 'ω'.

4. Concept of effective length of blockage (blockage integral)

To understand the idea of blockage integral, we turn to fig 2, which shows the streamlines of a hypothetical potential flow inside a tube with blockage.

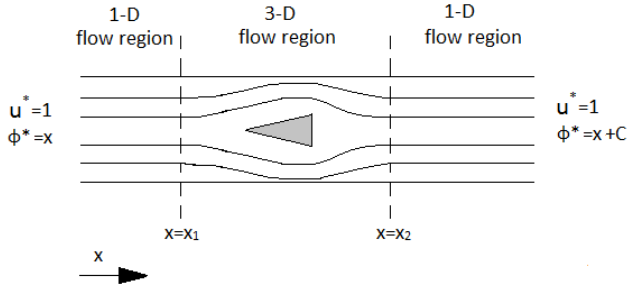

Fig 2: Different flow regions within a tube with blockage

As shown in fig 2, we divide the tube into three regions, such that the regions on either side of the blockage have a 1-D flow, with normalised velocity $u^*=1$, and corresponding velocity potential φ^*.

For $x<x_1$: $u^*=1$, $\varphi^*(x)=x$ (10)

For $x>x_2$: $u^*=1$, $\varphi^*(x)=x+C$ (11)

We now show that the integration constant 'C' is identical with the effective length L_{eff} in eq (5), which can be written in terms of the velocity potential φ (using $p=-\rho\partial\varphi/\partial t$):

$$-\varphi|_{x_1}+\varphi|_{x_2}=L_{eff}\,u|_{x_1} \quad (12)$$

Applying this to the potential flow shown in fig 2, we get

$$\varphi^*\big|_{x_2} - \varphi^*\big|_{x_1} = L_{eff} \tag{13}$$

The following expression for L_{eff} can be derived using matched asymptotic expansion [1,]

$$L_{eff} = \int_{-\infty}^{\infty} \left((\partial \varphi^* / \partial x) - 1 \right) dx \tag{14}$$

For numerical purposes, this is rewritten in terms of the stream function ψ^*, which is related to φ^* by (Cartesian coordinates).

$$\partial \varphi^* / \partial x = \partial \psi^* / \partial y \tag{15}$$

Also the integrand in (14) is zero for $x < x_1$ and $x > x_2$, so only a finite integration range is required.

$$L_{eff} = \int_{x_1}^{x_2} \left((\partial \psi^* / \partial y) - 1 \right) dx \tag{16}$$

The numerical calculation is done in two steps. First, the field $\psi^*(x, y)$ is calculated by solving its governing equation,

$$\partial^2 \psi^* / \partial x^2 + \partial^2 \psi^* / \partial y^2 = 0 \tag{17}$$

subject to the boundary condition that the normal velocity is zero on all the internal surfaces. A finite difference scheme, combined with a relaxation method, is used to solve (17) (see Press et al. section 17.5)[6]. In the second step, the streamlines are visualised and the integral in (16) is calculated with Simpson's 1/3rd integration rule.

The significance of blockage integral is that it simulates the 3-D hydrodynamic region around the blockage with a lumped inertia of infinitesimal extent located on a single hypothetical plane. Hence, our modified tube looks like fig 3. The tube has two acoustic regions upstream and downstream of the blockage.

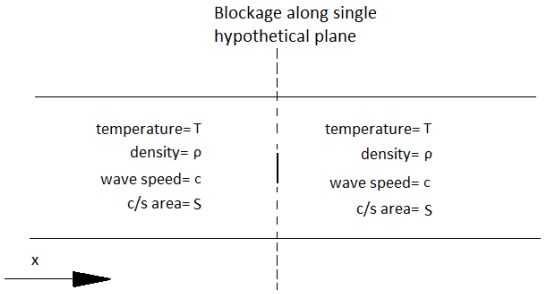

Fig 3: Representation of the blockage by a lumped inertia a single hypothetical plane

5. Blockage integral evaluation: two case studies

We are going to evaluate the stream functions for two special combustor models, one with high blockage and another with a low blockage. The schematic of the combustors are given below

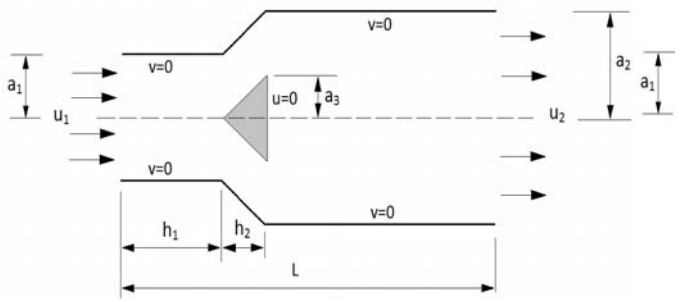

Fig 4a: Combustor with low blockage

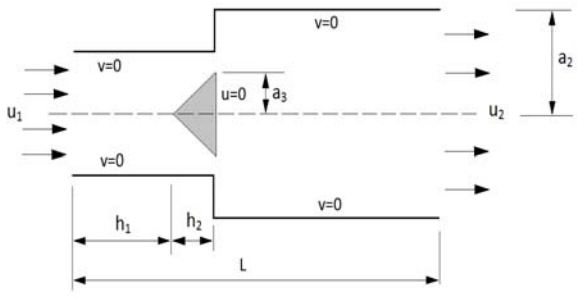

Fig 4b: Combustor with high blockage

The streamlines for the two combustors are shown in fig 5,

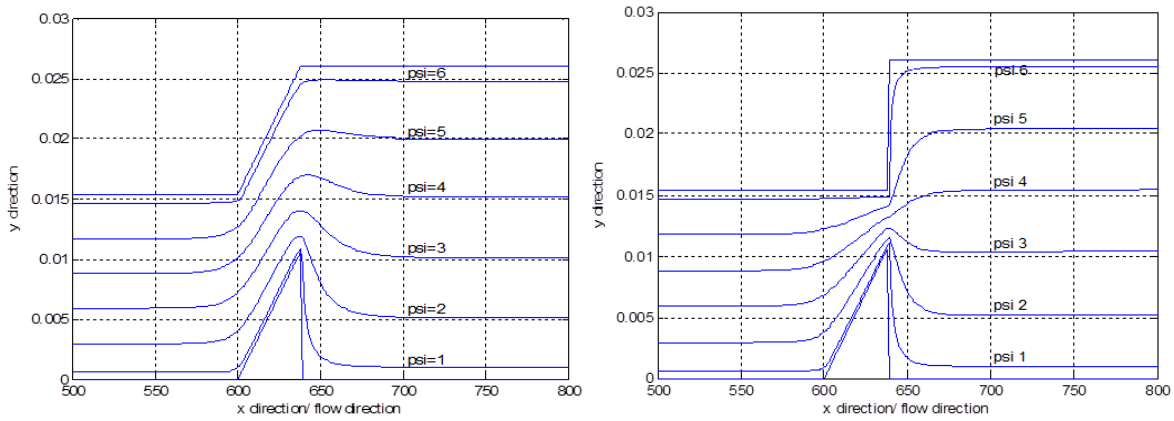

Fig 5: Streamlines for combustor with low and high blockage

The blockage integral calculated for the two combustor models are 0.115 m and 0.239 m respectively, using equation (14). Thus the blockage integral is a representative of the physical blockage within a tube.

6. Results showing the influence of blockage and area jump

6.1 Pressure profile within tube

In this subsection, we are going to demonstrate the acoustic pressure and velocity profile within the tube with blockage and area jump. Figure (6) and (7) represent sample plots of the acoustic pressure and particle velocity within the tube. In figure 6, the blockage is situated at $x_2 = L/4$, and in figure 7 at $x_2 = L/2$ (halfway along the tube). Comparison of the two figures shows that the effect of the blockage depends on its location along the tube axis. In figure 6, its location is between a pressure node ($x = 0$) and a pressure antinode ($x = L/2$). It causes the pressure jump, which appears in this figure. In figure 7, the blockage sits at a pressure maximum, and there it has no effect.

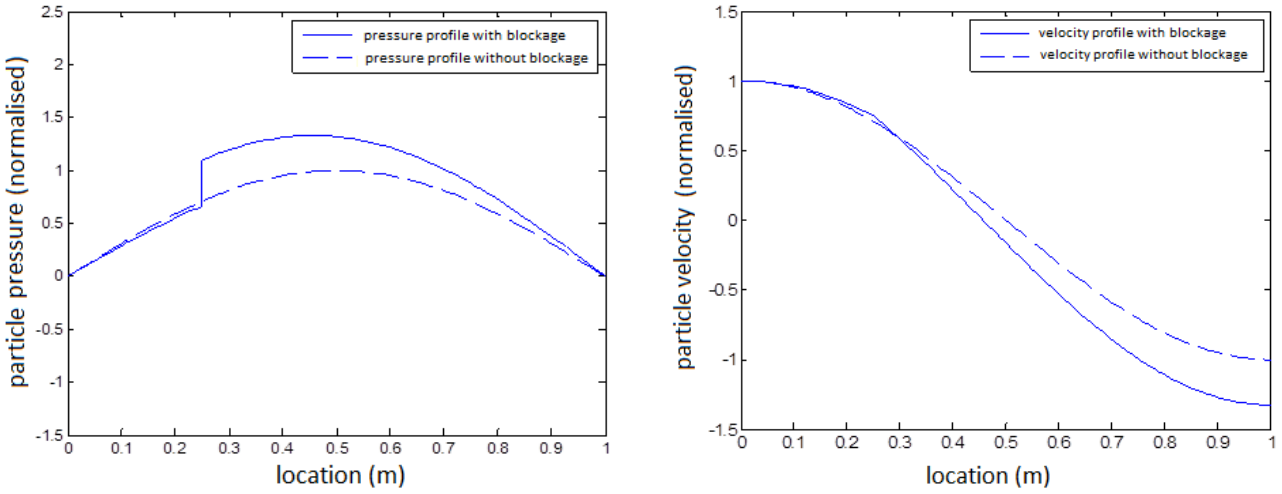

Fig 6: Pressure and velocity profile within tube for mode 1 at x_2=0.25L

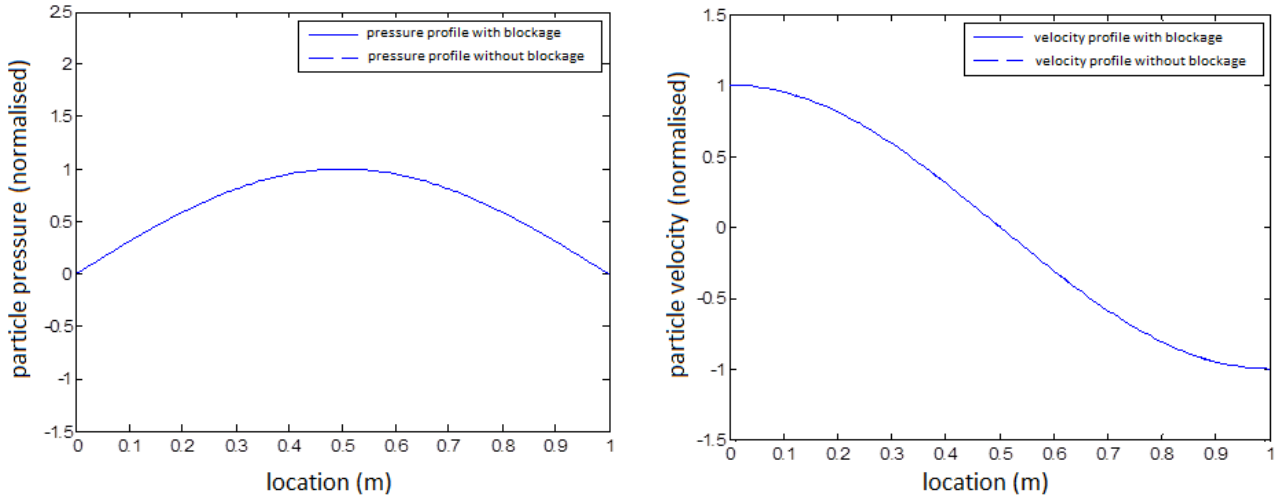

Fig 7: Pressure and velocity profile within tube for mode 1 at x_2 =0.50L

6.2 Effect of blockage integral on modal frequency

In this section we assume that there is no jump in the cross sectional area. The data assumed to generate the plots are as follows, L =1m, L_{eff} =0.2m, ρ =1.225 kg/m^3, c =340 m/s.

Figures (8) and (9) show how the frequency of the first two modes depends on the blockage integral. The results are shown for two different blockage locations: in figure 8, the blockage is at $x = 0.1m = 0.1L$, and in figure 9 it is at $x = 0.25m = 0.25L$. At each position, the blockage integral is varied from 0 m to 0.45 m. The trend of the plots is clearly visible to be decreasing for most of the cases. However, this trend is not visible for mode 2 in fig 9. At this position, the frequency of mode 2 is constant with respect to blockage.

Therefore, we can see that the modal frequency may go down or remain constant with respect to the blockage integral. The possible reason could be that the blockage integral represents similar effect of acoustic inertia and thus, as inertia increases the modal frequency decreases. However, at pressure antinodes, the acoustic particle velocity is 0. Therefore, from equation (5), we can say that pressure does not face any jump at $x = x_2$ and the blockage is ineffective at $x = x_2$. Hence, the modal frequency remains same as that of the case of a tube without any blockage at all.

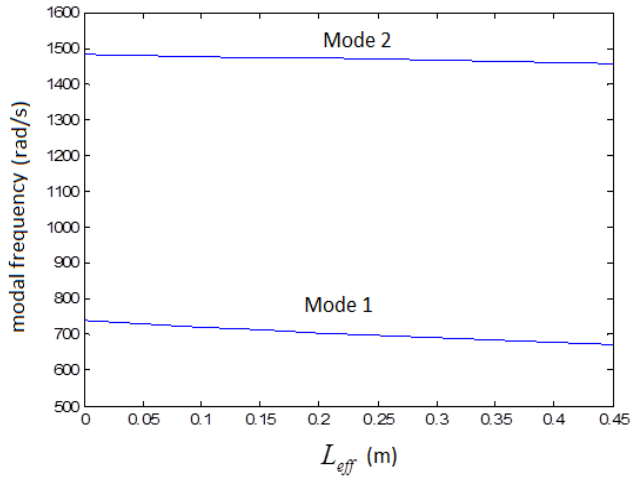

Fig 8: Blockage location, x_2 =0.10L

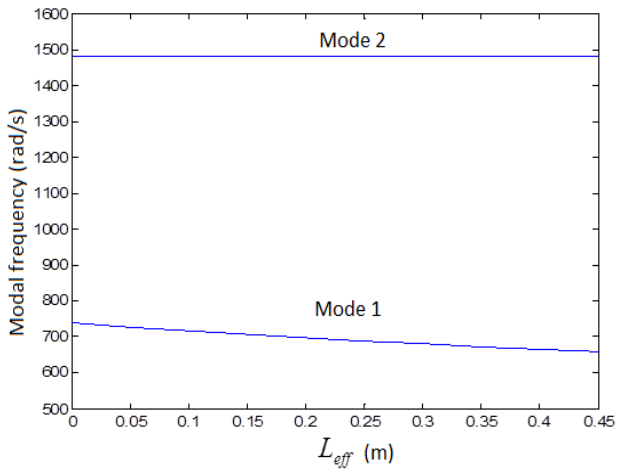

Fig 9: Blockage location, x_2 =0.25L

6.3 Effect of area jump on modal frequency

In this subsection, we are going to consider the change of modal frequency with respect to area jump. This subsection is based on the following assumptions,

1. Effect of blockage is neglected
2. Area jump is a step jump and not gradual

Figure (10) and (11) show how the modal frequencies depend on the size of the area jump. The ratio of cross-sectional area is varied between 0.25 and 2.5. The results are shown for two different jump locations: $x_1 = 0.1L$ (fig 10) and $x_1 = 0.35L$ (fig 11). From fig (10), we can see that the frequencies of both mode 1 and mode 2 are decreasing. The situation is different in fig 11, where the frequency of mode 1 decreases with the area ratio, while that of mode 2 increases. It has been also observed that at x=0.25m the frequency of mode 2 remains constant and at x=0.5m, the frequency of both mode 1 and mode 2 remains constant. In summary, the modal frequency may go up or down with respect to area jump, depending on the location of the jump within the tube. A detail study of this feature and its possible explanation will be provided in the following paragraph.

Fig 12 represents the pressure profile of mode 1 within the tube. It also explains that with respect to increased area jump the modal frequency decreases in the first half of the tube. In the second half of the tube, an increase in area jump leads to an increase in modal frequency. However, exactly at the tube centre, where mode 1 has a pressure antinode, the area jump does not alter the modal frequency. At the pressure antinode, particle velocity is zero. Therefore, equation (4) suggests that no matter what is the value of (S_2/S_1), the continuity equation is always satisfied and the modal frequency, thus, remains unchanged.

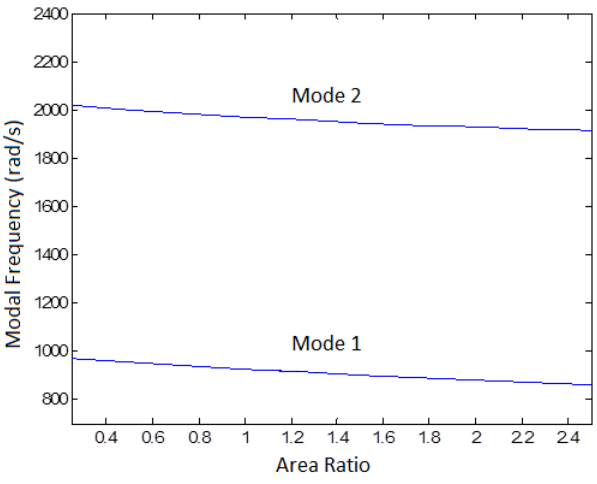

Fig 10: Area jump location, x_1=0.10L

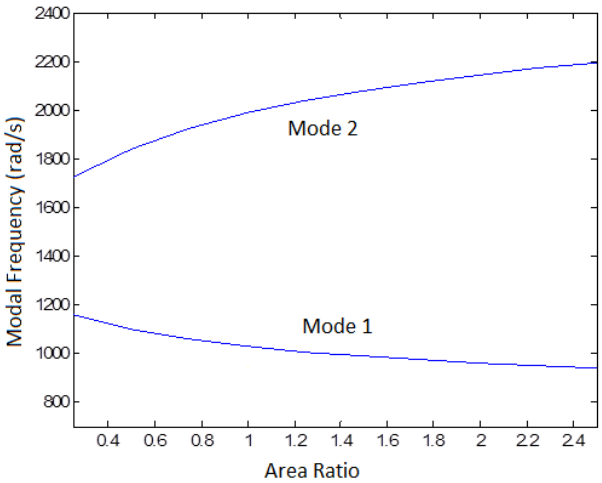

Fig 11: Area jump location, x_1=0.35L

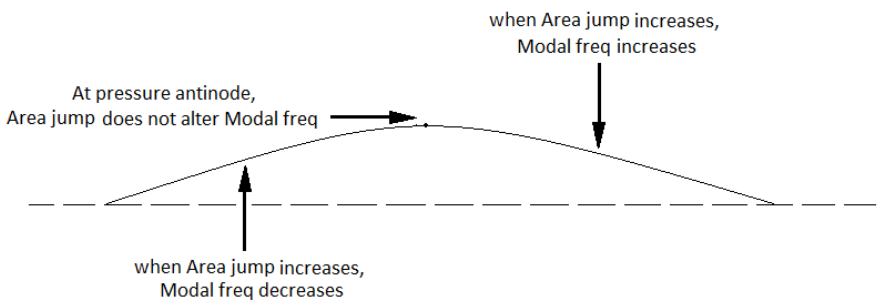

Fig 12: Effect of area jump on first mode (Boundary condition open-open)

7. Summary and outlook

The current work modelled the blockage and area jump within a tube, using the concept of the blockage integral. The modal frequency of the system was evaluated and the following features were identified:

1. The modal frequency decreases with increasing blockage size at all the locations in the tube except at a pressure antinode, where the modal frequency remains constant

2. The modal frequency may increase or decrease with respect to area jump depending on the location of the area jump within the tube. In zones of increasing pressure the modal frequency increases. The reverse trend is observed in zones of decreasing pressure. At a pressure antinode, the modal frequency remains constant.

The modal frequency analysis of the system using the concept of the blockage integral gives us a clear idea about how the blockage affects the acoustic field and modal frequency of a tube. This exercise could be extended for a case where there is a temperature jump in the tube. Further, the combined effect of blockage and area jump, at the same location within tube, can also be treated. As of now, we have not done any computational/experimental verification of our results. Thus the scope of future work includes verification of the results, as well.

8. Acknowledgements

The presented work is part of the Marie Curie Initial Training Network Thermo-acoustic and aero-acoustic nonlinearities in green combustors with orifice structures (TANGO). We gratefully acknowledge the financial support from the European Commission under call FP7-PEOPLE-ITN-2012

References

1. Heckl Maria A., Howe M.S., ‘Stability analysis of the Rijke tube with a Green’s function approach’, *Journal of Sound and Vibration* **305** , 672-688, (2007)
2. Murray P.R., Heckl Maria A., ‘Green’s function model for a rectangular Rijke Tube’, *ICSV-17*, Cairo, 18-22 July (2010)
3. Murray P.R., Howe M.S., ‘Compact Green’s function for a generic Rijke Burner’, *International Journal of Spray and Combustion Dynamics*, **Volume-3**, Number-3, (2011), Pages 191-208
4. Flohr P., Paschereit C.O., Ronn B. V., Schuermans B., ‘Using CFD for time delay modelling of premixed flames’, *ASME Turbo Expo 2001*, New Orleans, Lousiana, USA, June 4-7, (2001)
5. Flohr P., Paschereit C.O., Bellucci V., ‘Steady CFD analysis for Gas Turbine Burner Transfer functions’, *American Institute of Aeronautics and Astronautics Paper*, (2003)-1346.
6. Press W.H., Flannery B.P., Teukolsky S.A., Vetterling W.T., ‘Numerical Recipes: The Art of Scientific Computing’, *Cambridge University press*, (1986).